FINITE ELEMENT ANALYSIS OF NOTCH BEHAVIOR USING A STATE VARIABLE CONSTITUTIVE EQUATION

L.T. Dame, D.C. Stouffer and N. Abuelfoutouh
Department of Aerospace Engineering and Applied Mechanics
University of Cincinnati, Cincinnati, Ohio 45221

The state variable constitutive equation of Bodner and Partom was used to calculate the load-strain response of Inconel 718 at 649°C in the root of a notch. The constitutive equation was used with the Bodner-Partom evolution equation and with a second evolution equation that was derived from a potential function of the stress and state variable. Data used in determining constants for the constitutive models was from one-dimensional smooth bar tests. The response was calculated for a plane stress condition at the root of the notch with a finite element code using constant strain triangular elements. Results from both evolution equations compared favorably with the observed experimental response. The accuracy and efficiency of the finite element calculations also compared favorably to existing methods.

INTRODUCTION

The purpose of this work is to explore the development, efficiency and accuracy of a finite element computer code for hot section gas turbine components that is based on a state variable constitutive equation. The Bodner-Partom constitutive equation [1,2,3] used for this study, does not require the use of a yield surface or separate representations for loading and unloading in the elastic and inelastic domains. The model contains a single state variable to define the resistance to inelastic flow or hardness. This variable is determined from the deformation history in this study using two different evolution equations. The results from the evolution equation developed by Bodner and Partom and proposed with the flow equation are compared to the results computed from an evolution equation that is derived from the inelastic flow equation itself, [4,5]. The second formulation is established using a potential function that can be derived from the first law of thermodynamics.

One of the important aspects of this study is to test the tensorial or multidimensional characteristics of the Bodner-Partom flow equation. The material parameters for the study are determined from one dimensional tests (tensile, creep and fatigue) on Inconel 718 at 649°C. The equations are used to compute the response of a notched specimen using a plane stress finite element computer analysis. The calculated results for the strain in the root of the notch are compared to measured values reported by Domas et al in [6] for the same material. This provides a test of the model to predict the response in a general state of loading from data obtained in uniaxial experiments. A comparison that is usually difficult to achieve.

Another important aspect of this work is the development of the finite element computer code as a design tool and utilizes the state variable constitutive model. The code is based on two-dimensional constant strain triangles, an initial strain iterative procedure, piecewise linear load histories in a steady state thermal environment and a dynamic time stepping algorithm.

THE BODNER-PARTOM EQUATIONS

These equations were motivated by the concepts of dislocation dynamics and formulated in the context of mechanics. For small strains, the strain rates are considered to be decomposable into elastic, $\dot{\varepsilon}^e_{ij}$, inelastic, $\dot{\varepsilon}^I_{ij}$, and thermal, $\dot{\varepsilon}^T_{ij}$, components; that is

$$\dot{\varepsilon}_{ij} = \dot{\varepsilon}^e_{ij} + \dot{\varepsilon}^I_{ij} + \dot{\varepsilon}^T_{ij} \tag{1}$$

where $\dot{\varepsilon}^e_{ij}$ are given in terms of the stress rates determined from the time derivative of Hooke's Law and ε^T_{ij} is proportional to the change in temperature from a reference state. All components of Equations (1) are always nonzero for all nonzero values of stress and stress rate. However, the values of the inelastic strain rate term are negligible for small values of stress; thus, a yield criteria and separate loading and unloading representations are not required.

The inelastic strain rate is written in a form similar to the Prandtl-Reuss flow law; i.e.

$$\dot{\varepsilon}^I_{ij} = D_0 \exp\{-\frac{n+1}{2n}[\frac{Z^2}{3J_2}]^n\} \frac{S_{ij}}{J_2} \tag{2}$$

where D_0 is the limiting strain rate in shear. The material constant n controls the strain rate sensitivity and also influences the overall level of the stress-strain curves and J_2 is the second invariant of the deviatoric stress tensor, S_{ij}. The internal state variable, Z, governs the resistance to inelastic flow such that an increase in Z corresponds to work hardening and would require an increase in stress to maintain a constant inelastic strain rate.

The hardening law proposed by Bodner and Partom for application with several materials is

$$\dot{Z} = m(Z_1 - Z)\dot{W}^I - AZ_1(\frac{Z-Z_2}{Z_1})^R \tag{3}$$

where $Z = Z_0$ initially. The first term defines the rate strain hardening and $\dot{W} = S_{ij}\dot{\varepsilon}^I_{ij}$ is the inelastic rate of working. The second term in Equation (3) characterizes the thermal recovery and is important for

predicting creep. The representation is only for primary and secondary creep, and the secondary creep rate is obtained when $\dot{Z} = 0$. The constant Z_1 defines the maximum value of Z and Z_2 is the minimum value of Z obtained in thermal recovery. Frequently Z_2 is taken equal to Z_0; that is, the initial hardness and minimum recoverable value of Z are equal. Methods to determine the constants are presented in References [7] and [8], and the constants for Inconel 718 at 649°C are given in Table 1.

The model presented above, in addition to neglecting tertrary creep, is limited to an isothermal environment and isotropic hardening. An extension to time varying temperature histories is based on making n temperature dependent as reported in [3]. Extension to a hardening rate similar to kinematic hardening for uniaxial histories is given Reference [9]; but a full three dimensional anisotropic hardening law still needs to be verified for a variety of loading conditions.

A POTENTIAL FUNCTION DERIVATION

Recently it has been shown [4,5] that a system of equations to predict the inelastic strain rate and evolution of the state variables are derivable from a potential function. The essential structure of the theory is based on the balance law of thermodynamics and the concept of work hardening. For isothermal histories, the reduced form of the potential relationship is

$$\dot{\varepsilon}^I_{ij} = \frac{\partial \phi}{\partial \sigma_{ij}} \quad \text{and} \quad \dot{\mu} = \frac{\partial \phi}{\partial Z} \tag{4}$$

where ϕ is a function the stress and stress state variable, Z. The quantity μ is a strain on the microscopic scale such that $Zd\mu$ is the stored energy of cold work. The relationship between μ and Z on the microscopic scale is taken in the form of the Prandtl-Reuss equation on the macroscopic scale; i.e.

$$\dot{\mu} = g\dot{Z} + hZ \tag{5}$$

where g and h are generally assumed to be functions of σ_{ij} and Z but are taken as constants in this study. Combining Equations (4) and (5) and redefining the constants as α and β gives

$$\dot{Z} = -\alpha(Z-\xi) + \alpha\beta I \tag{6}$$

where ξ is a material parameter. The quantity I is the integral

$$I = \frac{1}{|\dot{\underline{\varepsilon}}^I|} \int_o^t \frac{\partial \dot{\varepsilon}^I_{ij}}{\partial Z} d\sigma_{ij} \tag{7}$$

where $|\dot{\underline{\varepsilon}}^I| = (\dot{\varepsilon}^I_{ij}\dot{\varepsilon}^I_{ij})^{1/2}$ and $\dot{\varepsilon}^I_{ij}$ is evaluated using the Bodner Partom Equation in this example.

The parameter α characterizes the initial rate of hardening, $\dot{Z}_0$, which arises from the integration. This term contributes to the strain rate sensitivity of the model and includes the initial loading such as in a creep

test [4]. For this exercise α is taken as $125|\dot{\varepsilon}_0|$. The remaining parameters ξ and β can be calculated directly from creep or tensile data during steady state conditions; that is, when both the strain rate and stress are approximately constant. In this case $\dot{Z} = 0$ and Z obtains a steady value, Z_s, that depends on the test conditions. A plot of Z_s vs I for Inconel 718 at 649°C shows that this response is nearly trilinear and can be represented by the parameters shown in Table 1.

FINITE ELEMENT IMPLEMENTATION

The finite element code utilizes two dimensional constant strain triangles and an initial strain iteration technique. To facilitate the simulation of arbitrary load histories, the load history is partitioned into piecewise linear segments. In order to simplify input, reduce stability problems and minimize cost a dynamic time stepping procedure is also incorporated.

The incremental equilibrium equation for the initial strain method with steady state thermal conditions is

$$[K]\{\Delta d^T\} = \{\Delta F\} + \{\Delta F^I\} \tag{8}$$

where [K] is the elastic stiffness matrix, $\{\Delta d^T\}$ is the increment in the total displacement vector, $\{\Delta F\}$ is the increment in the applied force vector and $\{\Delta F^I\}$ is a pseudo force vector due to the increment in a vector of the inelastic strains components. The vector $\{\Delta F^I\}$ is calculated by

$$\{\Delta F^I\} = \sum_1^N \left(\int_v [B]^T[E]\{\Delta \varepsilon^I\}dv\right) \tag{9}$$

where N is the number of elements. In Equation (9), [B] is the strain displacement matrix and [E] is the elastic constitutive matrix.

At the beginning and end of a linear load case the elastic solutions are obtained using

$$\{d^E\}_0 = [K]^{-1}\{F\}_0$$

and

$$\{d^E\}_F = [K]^{-1}\{F\}_F \; . \tag{10}$$

The vectors $\{d^E\}_{0,F}$ are the initial and final elastic displacements due to initial and final applied thermomechanical loads. The elastic displacements at any time t_i in the load case are given by

$$\{d^E\}_i = \{d^E\}_0 + \frac{t_i - t_0}{t_F - t_0}\left[\{d^E\}_F - \{d^E\}_0\right]. \tag{11}$$

The total displacement vector at time t_i is written as

$$\{d^T\}_i = \{d^E\}_i + \{d^I\}_{i-1} + \{\Delta d^I\} \tag{12}$$

where the increment in the inelastic displacement vector is

$$\{\bar{\Delta d}^I\} = [K]^{-1}\{\Delta F^I\} \tag{13}$$

and the increment in the inelastic pseudo force vector is given by Equation (9). Thus, it is necessary to integrate the constitutive model from time t_{i-1} to t_i. Although any number of integration schemes could be used, a second order Adams-Moulton method was employed. Since the flow equation and the state variable evolution equation are coupled an iterative procedure is required to compute $\{\dot{\varepsilon}^I\}$ and $\dot{Z}$ at the end of a time step. The integration of the constitutive equation is within the overall equilibrium iteration loop as shown in Figure 1.

A significant improvement in the iteration scheme was achieved by making an initial estimate of the incremental inelastic pseudo force vector $\{\Delta F^I\}$ in the first iteration of a new time step. If $\{\Delta F^I\}$ is set equal to zero on the first iteration of a new time step (as is usually done) the first estimate of the solution may be very poor. An initial estimate of the inelastic strain increment for each element can be made using $\{\Delta \varepsilon^I\} = \{\dot{\varepsilon}^I\}_{i-1}\Delta t$, where $\{\dot{\varepsilon}^I\}_{i-1}$ is the inelastic strain rate at the beginning of the time increment. If this is then used in Equation (9) to make an initial estimate of the incremental inelastic force vector the stability and rate of convergence of the method is improved. By including this logic, the number of equilibrium iterations was reduced by about 60%.

In a finite element code that allows a linear variation of applied loads, large excursions in stress and inelastic strain rate are to be expected. To be economical and easy to use, dynamic time incrementing is a necessity. There are two important considerations in developing such an algorithm; first the stability of the iteration scheme and second the accuracy of the integration procedure. The stability of the system of equations depends on the constitutive model, geometry, loading history and material parameters. An approximate but simple and effective approach is to base the time step on the maximum inelastic strain increment to occur in all of the elements. In order not to overshoot the point where inelastic strain rates become significant it is also necessary to limit the maximum stress increment. A final consideration is controlling the local integration error when computing inelastic strain increments. For components in which fatigue life is a major consideration the accurate calculation of local stresses and strains is crucial. In order to control the error the time step should be chosen such that the local integration error does not exceed some allowable value.

CALCULATED AND EXPERIMENTAL RESULTS

A recent comprehensive study, [6], of the strain in the root of a notch was conducted for a variety of local patterns in Inconel 718 notch specimens at 649°C (1200°F). A laser interferometric strain displacement gage was used with reasonable certainty to evaluate the displacement of a gage 100 microns in length at the root of the notch at temperature. The

measurements were made for six load histories including continuous cycling and cycling with hold time periods in tension, tension and compression, and compression. The specimen was a thin flat double notch bar, as shown in Figure 2, with an elastic stress concentration factor of 1.9. The geometry in the test section is approximately plane stress and is modeled by the constant strain triangular element mesh also shown in Figure 2.

The above study included a limited number of smooth bar tests in tension, creep and cycling for use with a Neuber analysis. These data and other published tensile, [10], and creep, [11], data were used to evaluate the material parameters in the flow and evolution equations. The constants were evaluated using the methods reported in [4], [7] and [8]. The major difficulty encountered was not having two complete tensile curves at different strain rates to evaluate the parameter n in the inelastic flow equation. Thus an estimate was used based on one curve and the other constants, as shown in the Table 1, were evaluated based on this value. Increases in n would change the values of the other parameters, but the combined effect would produce essentially the same predictions with less strain rate sensitivity in the tensile response. Decreases in n would cause the equations to overpredict the tensile strain rate sensitivity.

The calculated response to a smooth bar tensile test at a strain rate of one percent per minute is shown in Figure 3a for the two evolution equations. The potential function representation overpredicts the observed stress in the transition from elastic to plastic response; however the asymptotic behavior of both representations match the data very well. The calculated smooth bar creep response is shown in Figure 3b for three values of stress. The results of the calculations are mixed with the potential function representation better at the high value of stress, the Bodner-Partom representation better at the intermediate value of stress and both models underpredicting the creep strain at lower values of stress. In general, representations could be improved by adjusting the material parameters; however, with only five curves in the smooth bar data base there is no guarantee that this would improve the predicted response of the notch strain. The flow law is also limited to primary and secondary creep, so no correlation with the tertiary creep is included.

The strain response at the root of the notch for three tests is shown in Figures 4, 5 and 6. The total specimen load is held constant for two minutes in compression, tension and compression, and tension as shown in Figures 4, 5 and 6, respectively. The finite element and experimental results are for the first cycle. In general, both evolution equations match the measured data rather well. The largest error is the over prediction of the tensile creep in Figure 6 by both equations; however, the measured tensile creep in Figure 6 is much less than the measured tensile creep in Figure 5 where the predictions are satisfactory. The assumption of isotropic hardening appears reasonable for the first cycle and the correlation with compressive creep is shown in Figures 4 and 5.

DISCUSSION

The state variable constitutive models used in this study have several advantages and limitations. The formulation is convenient for finite

element methods, because it admits a forward time marching integration procedure and does not require separate loading and unloading representations. The flow law and evolution equation can predict many inelastic effects; however, for Inconel 718 there still are some areas that need improvement. Inconel 718 general exhibits a combination of "kinematic and isotropic" hardening and softening in uniaxial cycling which is not included in the current formulation. Further, the constitutive models have not been fully developed and verified for nonisothermal loading conditions. For extension to multiple cycle analysis it would also be advantageous to use the cyclic stress-strain curve rather than the monotonic response curve to determine the material parameters.

There is a correlation in the errors observed in the calculated finite element response at the root of notch and the smooth bar calculated response. When using the Bodner-Partom evolution equation, (3), the creep strain at 827MPa(120KSI) was over predicted. The calculated tensile creep response in the root of the notch is largest for the Bodner-Partom equations as shown in Figures 5 and 6. This observation indicates that the finite element predictions could be refined by improving the smooth bar calculated response. Recalling that the constitutive parameters were obtained from five curves, one tensile and four creep published [6,10,11] between 1971 and 1982, the calculations are reasonable and could be improved by improving the smooth bar data base.

The computational exercises were limited to initial cycle of three load patterns for reasons of cost and lack of cyclic data to develop the model. The computational efficiency proved to be very good. On a Honeywell 6000 computer, the run times varied from 1.5 to 3.5 CPU hours for a model with over 1000 elements. This is very competitive with similar finite element calculations based on classical plasticity and creep formulations. Further, the longest time could have been reduced by incorporating all the time saving features used in the later runs.

ACKNOWLEDGEMENT

The authors thank the National Aeronautics and Space Administration for their support under grant NAG 3-511 to the University of Cincinnati, Cincinnati Ohio and Contracts NAS3-23698 and NAS3-23927 to the Aircraft Engine Business Group, General Electric Co., Evendale Ohio.

REFERENCES

[1] Bodner S.R. and Partom Y., "A Large Deformation Elastic Viscoplastic Analysis of Thickwalled Spherical Shells," Journal of Applied Mechanics V39, pp 751-757 (1972).

[2] Bodner S.R. and Partom Y., "Constitutive Equations for Elastic Viscoplastic Strain Hardening Materials," Journal of Applied Mechanics V42, pp 385-389 (1975).

[3] Bodner S.R., Partom I and Partom Y., Journal of Applied Mechanics, V46, pp 805-810 (1979).

[4] Abuelfoutouh N.M. "A Thermodynamically Consistent Constitutive Model for Inelastic Flow of Materials," Ph.D. Dissertation, University of Cincinnati 1983.

[5] Stouffer D.C. and Abuelfoutouh N.M., "A Potential Function Constitutive Equation for Inelastic Material Response," NASA Conference Publication 2271, pp 153-177 (1982).
[6] Domas P.A., Sharpe W.N., Ward N. and Yau J., "Benchmark Notch Test for Life Prediction," NASA CR-165571, 1982.
[7] Stouffer D.C. and Bodner S.R., "A Relationship Between Theory and Experiment for a State Variable Constitutive Equation," American Society for Testing and Materials, ASTM-STP765, pp 239-250 (1982).
[8] Nicholas T., "Finite Element Analysis of Cracked Bodies Using the Bodner-Partom Flow Law," 2nd Symposium of Nonlinear Constitutive Relations for High Temperature Application, NASA Lewis Research Center, June 1984.
[9] Stouffer D.C. and Bodner S.R., "A Constitutive Model for Deformation Induced Anisotropic Plastic Flow of Metals," International Journal of Engineering Science, V17, pp 757-764 (1979).
[10] Brinkman C.R. and Korth G.E., "Strain Fatigue and Tensile Behavior of Inconel 718 at Room Temperature to 650°C," Journal Testing and Evaluation, 2.4, pp 249-259, July 1974.
[11] NIR (Kushnir) N, Eylon D. and Rosen A., "The Effect of Rapid Thermal Fluctuations on the Creep Rate in Inconel 718," Metallurgical Transactions, 2, pp 2237-2241, Aug. 1971.

Table 1. Constitutive Parameters

Flow Equation:

$D_0 = 10^4 SEC^{-1}$ $\quad n = 1.954$

Bodner Partom Evolution Equation:

$Z_0 = 1805MPa$ (262 KSI) $\quad A = 5.6 \times 10^{-5} SEC^{-1}$

$Z_1 = 2253MPa$ (327 KSI) $\quad M = 0.160MPa^{-1}$

$Z_2 = 1805MPa$ (262 KSI) $\quad R = 1.37$

Potential Function Evaluation Equation:

$Z_0 = 1860MPa$ (270 KSI) $\quad \alpha = 125|\dot{\varepsilon}_0|$

$|\dot{\varepsilon}^I| \leq 3.2 \times 10^{-10} SEC^{-1}$ $\quad \zeta = 0$

$\beta = 4.01 \times 10^7 MPa/SEC (5.82 \times 10^6 KSI/SEC)$

$|\dot{\varepsilon}^I| > 3.2 \times 10^{-10} SEC^{-1}$ and $\quad \zeta = -4033MPa(-585$ KSI)

$|\dot{\varepsilon}^I| \leq 7 \times 10^{-6} SEC^{-1}$ $\quad \beta = 1.60 \times 10^8 MPa/SEC (2.33 \times 10^7 KSI/SEC)$

$|\dot{\varepsilon}^I| > 7 \times 10^{-6} SEC^{-1}$ $\quad \zeta = 1102MPa(160$ KSI)

$\beta = 2.94 \times 10^7 MPa/SEC (4.27 \times 10^6 KSI/SEC)$

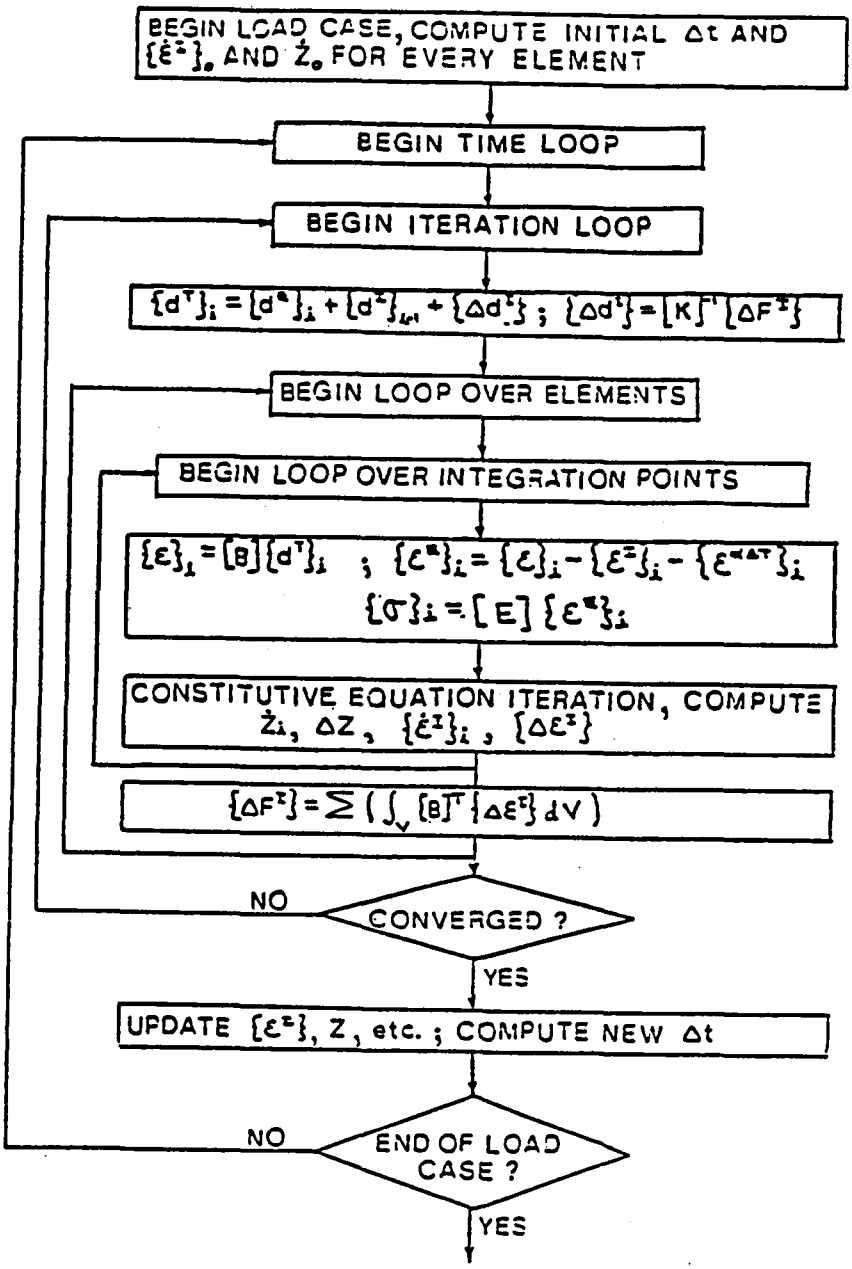

Figure 1. Schematic diagram of the iteration procedure for the finite element program.

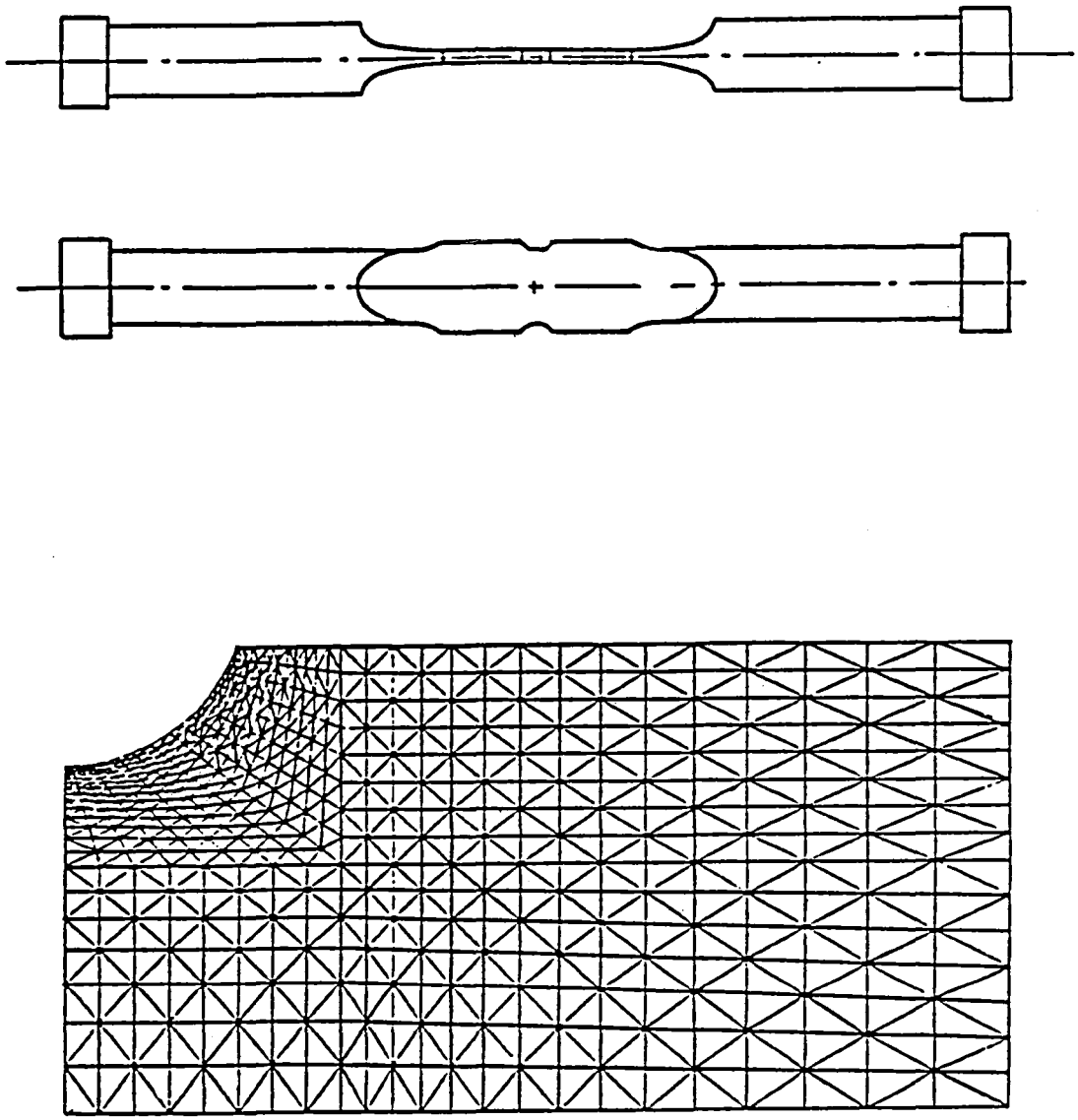

Figure 2. Description of the benchmark notch specimen and the finite element mesh at the root of the notch.

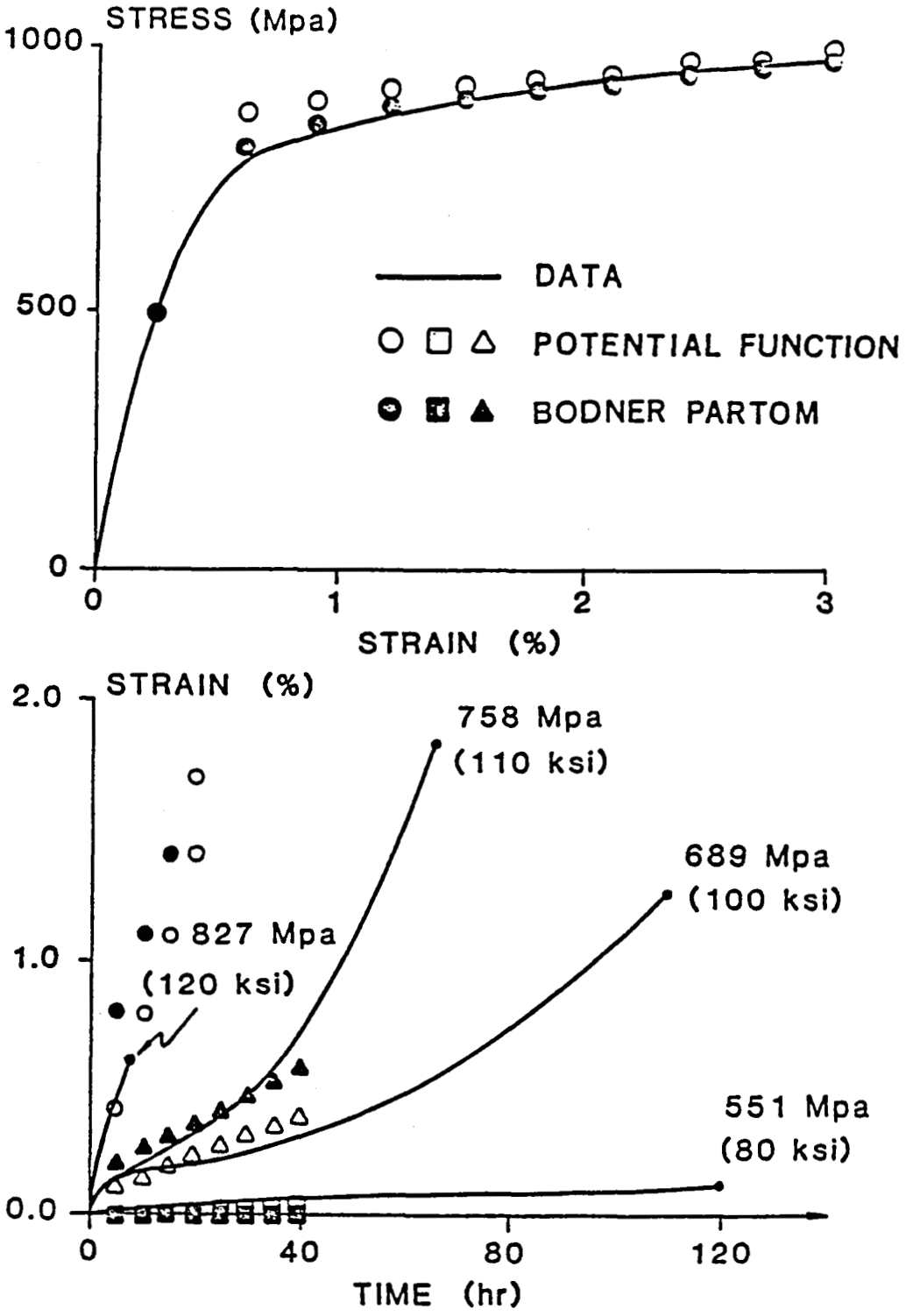

Figure 3. Comparison of experimental and calculated response of Inconel 718 at 649°C using the Bodner-Partom and potential function evolution equations: (A) tensile response at 1% per minute and (b) comparison of creep response at 689MPa(100KSI), 758MPa(110KSI) and 827MPa(120KSI).

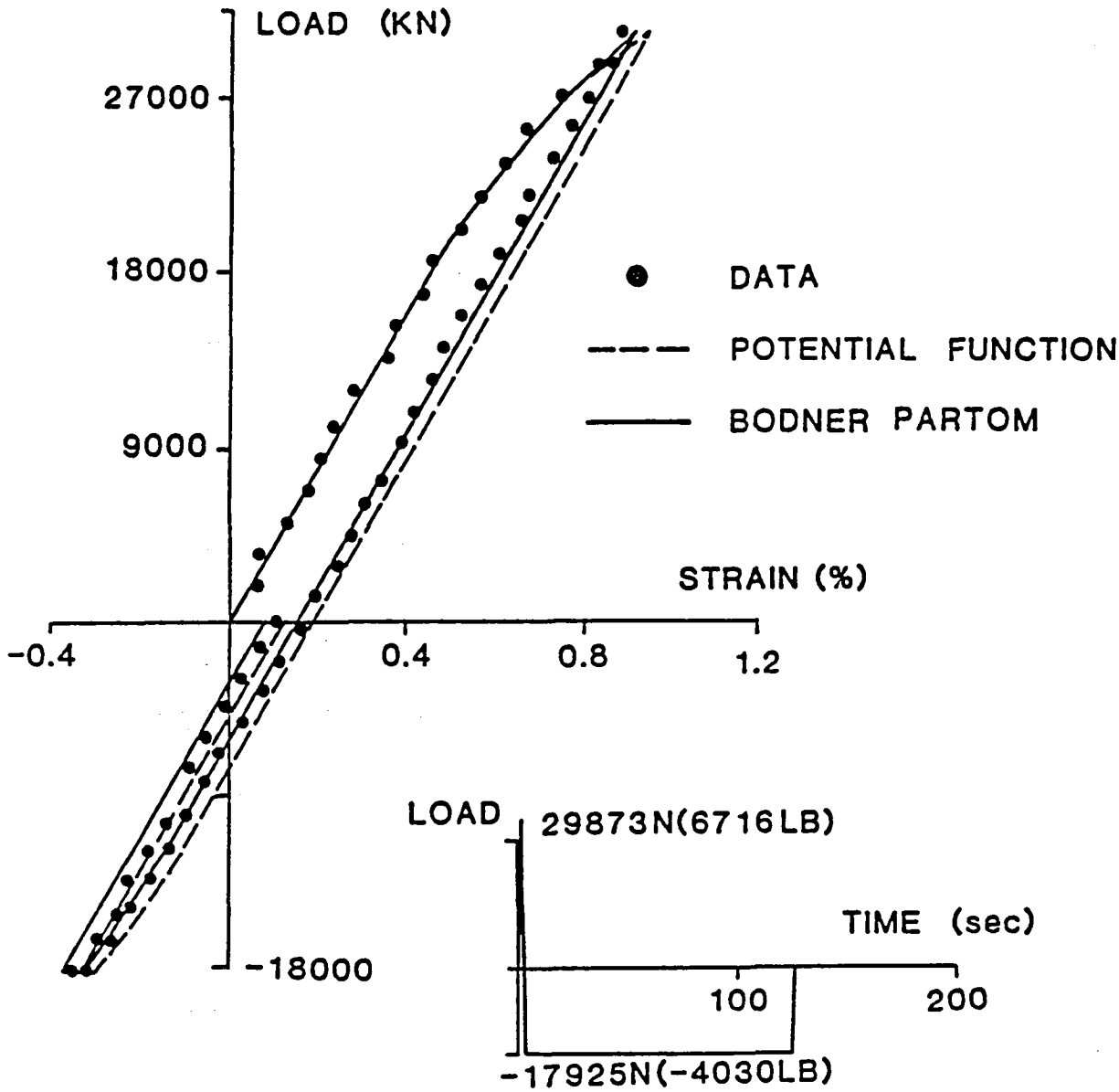

Figure 4. Comparison of experimental and calculated load-strain response at the root of the notch for Benchmark Notch Test 8 with a hold in compression.

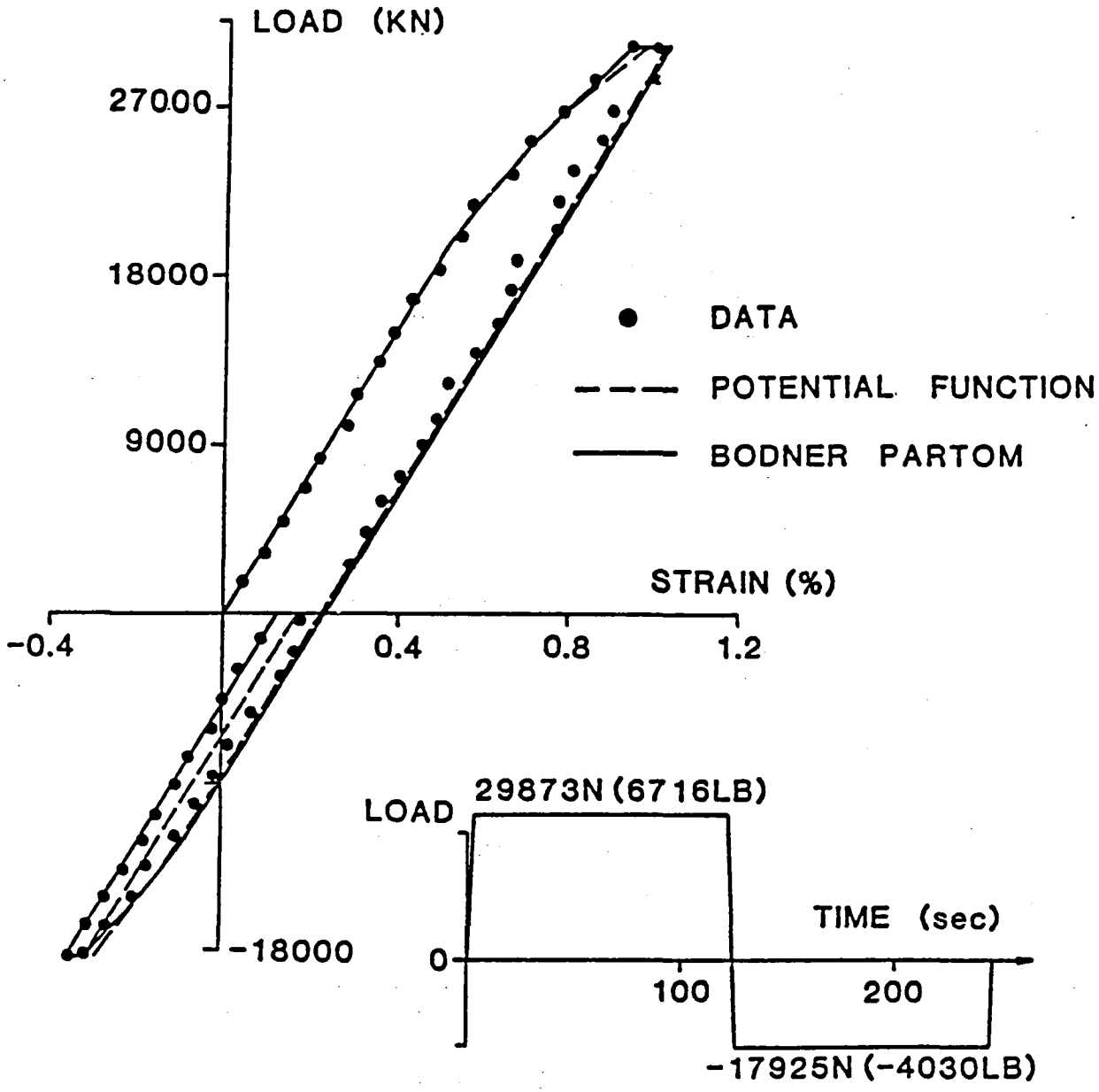

Figure 5. Comparison of experimental and calculated load-strain response at the root of the notch for Benchmark Notch Test 9 with hold in tension and compression.

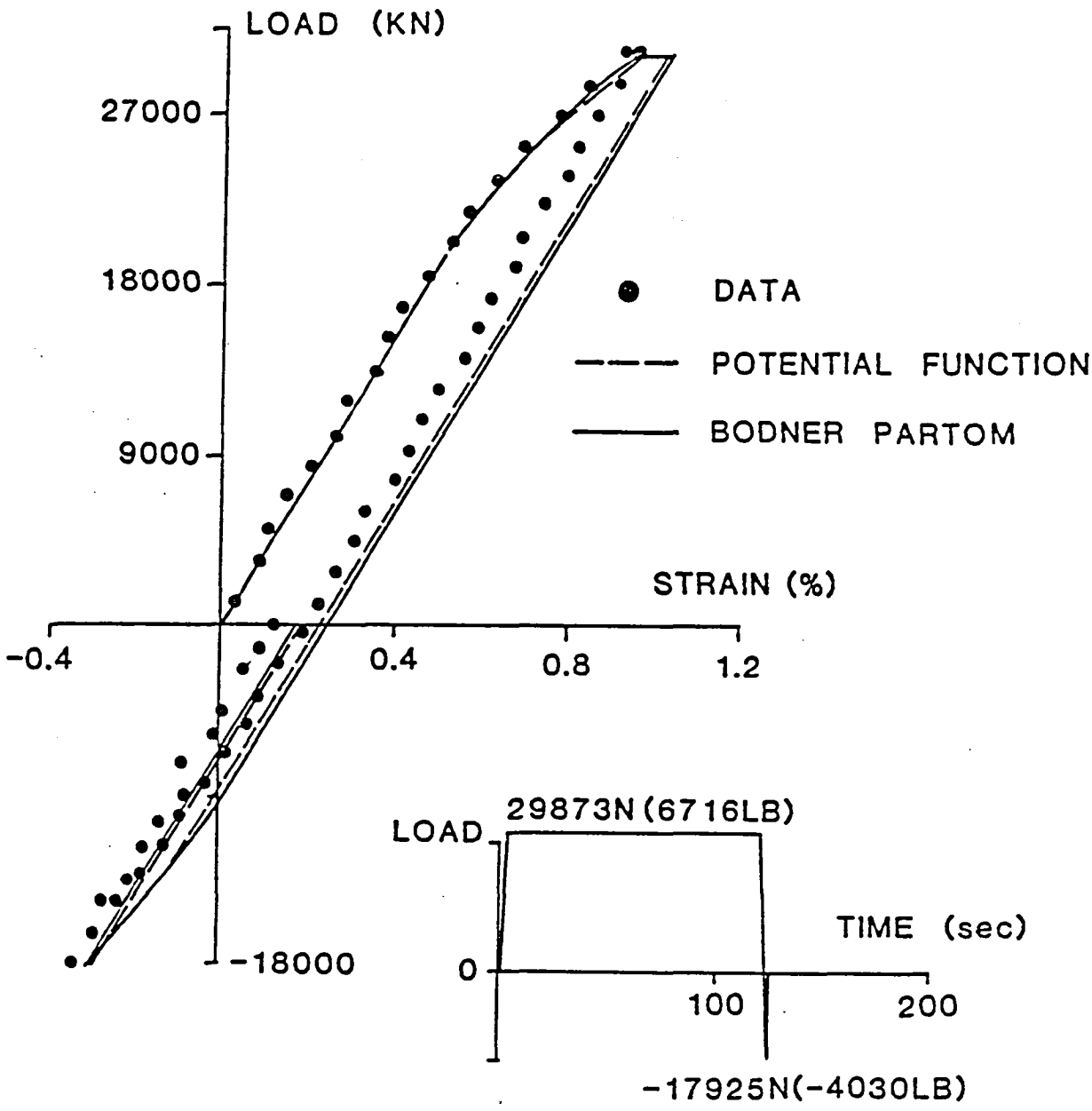

Figure 6. Comparison of experimental and calculated load-strain response at the root of the notch for Benchmark Notch Test 10 with hold in compression.